Influence of the freeze and thaw cycles in the physical and mechanical properties of granites

L. Martins[1], G. Vasconcelos[2], P.B. Lourenço[3], C. Palha[4]

[1] *PhD student, ISISE, Department of Civil Engineering, University of Minho, Azurém, P-4800-058 Guimarães, Portugal. Tel: +351 253 510 200, Fax: +351 253 510 217*

[2]*Assistant Professor, ISISE, Department of Civil Engineering, University of Minho, Azurém, P-4800-058 Guimarães, Portugal. Tel: +351 253 510 200, Fax: +351 253 510 217*

[3] *Professor, ISISE, Department of Civil Engineering, University of Minho, Azurém, P-4800-058 Guimarães, Portugal. Tel: +351 253 510 200, Fax: +351 253 510 217*

[4] *Civil Engineer, Department of Civil Engineering, University of Minho, Azurém, P-4800-058 Guimarães, Portugal. Tel: +351 253 510 200, Fax: +351 253 510 217*

Corresponding author: *graca@civil.uminho.pt*

Abstract

Vernacular built heritage in stone masonry remains and it is an evidence of the cultural and historical values. Therefore, it is important to preserve the stone of these buildings to harmful environment conditions like freeze-thaw and salt crystallization cycles, air pollution, excessive and frequent rain or snowfall, which can lead to decay processes which endanger the future of architectural heritage. For this, it is important to understand how environmental actions act on the physical and mechanical properties of building stones. In Portugal the most used building stone, particularly in the north region, is the granite, both in the vernacular and historical buildings.

Therefore, this research aims at evaluating the performance of different types of granite, characteristic of the northeastern region of Portugal to the action of freeze-thaw cycles, for which this environmental action is relevant, given the wide temperature range and the possibility of occurrence of negative temperatures. Frost resistance is important for the durability of the building stone since the freezing-thawing cycles of the water inside the stone pores results in development of internal stresses, which can lead to cracking and progressive desegregation of material. The analysis of the influence of the freeze and thaw environmental action in the granites belonging to Portuguese vernacular buildings was carried out, based on an enlarged experimental program for the obtainment of the physical and mechanical properties of distinct types of granites before and after the freeze and thaw cycles.

The present paper presents the experimental campaign of freeze-thaw cycles on three types of granites and discusses the main results analysing the standard damage indexes associated to the weathering process. Additionally, an analysis of the physical and mechanical properties and the variation of the ultrasonic pulse velocity (UPV) are provided. The freeze-thaw tests showed a considerable influence on the physical properties of granites. The UPV, dry mass and compressive strength decrease as the result of the material breakdown. The porosity of the

granite presents values significantly higher after the cycles of freeze-thaw, which also leads to the increased on the absorption by immersion and capillary absorption coefficient.

Keywords: granite, freeze and thawing cycles, physical and mechanical properties, UPV

Introduction

The deterioration of stone after freeze–thaw cycles is an important matter for natural building stones used in cold regions exposed to excessive freezing and thawing during the year. The assessment of stone deterioration due to environmental actions is an essential task for preservation and conservation purposes. For the quantification of deterioration, a fundamental understanding of stone weathering mechanisms and their influence on stone structure is necessary. Weathering processes can affect the physical and mechanical properties of stone and induce several changes in its structure, such as modification of porosity and pore structure, development of cracks and loss of stone cohesion. The study of these changes and the correlation of stone properties in different weathering conditions with easily measurable quantities help to develop classification schemes, whereby the deterioration level of stone can be assessed (Nicholson, 2001; Benavente et al., 2004; Tugrul, 2004).

The weathering induced by the action of freeze-thaw cycles associated to extreme environmental conditions results from many mechanisms associated to the change water state into rock voids. In the early nineteenth century some engineers had planned experiences about the decay of rocks by the action of ice. However, they used the crystallization of salts as the method of simulating the action of the ice, as made in the pioneering work of Evans (1970). With this respect, several studies are available in literature reporting the explanatory mechanics involved in aging of materials subjected to freeze-thaw and saline crystallization, both individually and in a combined way. It has been agreed that the main mechanism of degradation results from the development of internal hydraulic pressure, attributed to ice crystallization inside the material (Evans, 1970; Powers, 1945). This phenomenon was demonstrated in 1961 by Everett (1961), known as Taber-Everett effect. The Everett model´s suggests the importance of microcracking on the connection between larger pores. The comprehension of the deterioration phenomenon resulting from the action of freeze-thawing has deserved a closer

look of the scientific community due to the complexity of the variables involved, such as, the properties of water near the point of gelation, the gelation process and the properties of the ice. The phenomenon of freezing-thawing has also been extensively studied in concrete because it is a material commonly used in built patrimony. Tensions that repeatedly increase and decrease during the formation of successive layers of ice results in the fracture of the material (Chatterji, 1999). According to Scherer (2000), the crystallization pressure resulting from formation of ice in the pores consists of the main reason for the concrete degradation, which was demonstrated by the pressure developed by the crystallization of salts and ice against the pores walls of the material. However, there has been a contestation of the principle of crystallization pressures on freezing process as the basis for degradation of concrete. The pressure exerted by the water, which is enclosed in the icing, is considerate more important than the super cooling phenomenon that occurs in nature (Chatterji, 2000).

The action of freezing in materials like rocks depends on their physical properties, where the porosity degree and pores network determine the infiltration of the water and further positioning of ice in porous body. The temperature has been pointed out as the most important variable in the freeze-thaw process, followed by the transport properties of water and finally by the mechanical effects (Matsuoka, 1991). In fact, the geometry of the porous network influences the critical temperature, permeability controls the transport of water, and porosity influences the volumetric expansion and the consequent ice expansion stresses. The resistance to the ice in the form of dendrites inside the pores is conditioned by the mineralogical composition and pore spatial arrangement as the pore size determines the volume of ice crystals (Exadaktylos, 2006).

Recently, several works were carried out to study the resistance of rocks to freeze–thaw cycles (Maurenbrecher et al., 2005; Gao Pei-wei et al., 2006; Shang et al., 2008; Vegas et al., 2009; Pospíchal et al., 2010; Uddin et al., 2010; Martínez-Martínez et al., 2013). These researches

indicated that a minimum number of freeze–thaw cycles of 100 should be considered in order to guarantee that a considerable decay develops in the samples. The assessment of the influence of the freeze-thaw cycles was studied based on several physical properties namely, volume loss, open porosity variation, visual damage progress, water capillarity variation and ultrasonic pulse velocity. It was found that a linear relation exists between the of strength loss with the mass loss subjected to cycles of freezing and thawing. In relation to mechanical properties (strength and elastic modulus), it was observed that the uniaxial compression strength reduction is an important parameter indicating the deterioration due to freeze-thaw cycles (Bayram, 2012).

Frost weathering has been discussed as a major physical deterioration process. Freeze and thaw cycles are probably responsible for most damages in natural building stones during the winter, limiting their durability. Taking into account that the daily temperature amplitudes are very different in some days in the winter in the Northeastern region of Portugal, where great part of the vernacular construction was built in granitic stone, it is important to assess the vulnerability of this material to this type of environmental action. From an in-situ survey, it was possible to identify granular disintegration of the stone blocks from outside masonry façades of old masonry stone buildings (centenary houses) in Foz Tua valley, in the northeastern region of Portugal. Aesthetically, stone buildings exhibit a textured and aged color. Some rocks appeared so deteriorated that probably can disintegrate during next years. The degradation of stone building materials due to the variation of climatic conditions was also observed in other types of building stone, such as limestone in monuments in Austria, with alveolar form weathering, granular disintegration and efflorescence (Alomari et al., 2013).

Therefore, the present paper presents an experimental campaign of freeze-thaw tests on three distinct types of granites, which are characteristics of vernacular construction from northeastern region of Portugal, and discusses the main results associated to the weathering process of the granites. The assessment of the weathering of the granites to freeze-thaw cycles is carried out

based on the damage indexes proposed by European standard and, additionally, on the variation of physical properties, namely porosity, water immersion by immersion, water capillary absorption and ultrasonic pulse velocity. The compressive strength and elastic modulus were also compared before and after the maximum number of freeze-thaw cycles.

Experimental campaign

Given that the main aim of this paper is the obtainment the frost resistance and the assessment of the influence of the freeze and thaw cycles on the physical and mechanical properties of granites used in vernacular buildings, an experimental campaign based on freeze and thaw tests on different types of granites was designed. Physical and mechanical tests were also carried out for physical and mechanical characterization of granites before and after the imposition of the freeze and thaw cycles.

Materials

The granites adopted in the present work were collected from the northern region of Portugal. According to the information given in Table 1, three types of granites were considered, namely: (1) the granite designated by MDB, which is medium-grained two-mica granite. Two directions were considered for this granite, namely the direction parallel to the foliation plan and the direction perpendicular to the foliation plane. The foliation is given by the orientation of the biotite minerals; (2) the granite designated by PTM, which is a fine to medium-grained two-mica granite; (3) the granite FT, which is a fine to medium-grained two-mica granite. Contrarily to the granites MDB and PTM, which were taken from two distinct quarries, the granites FT was gathered from an abandoned vernacular construction from the Tua Valley, in the northeastern region of Portugal, which is very close to the Douro region. The idea was to characterize the typical granite found in different vernacular constructions of Tua Valey

as some of them will be submerged in the sequence of the dam built in the Tua river. A brief and simplified petrologic description of the granites is shown in Table 1.

Equipment

For the freeze-thaw tests, it was decided to use an adapted freezer so that the conditions of testing defined in the European standard EN 12371 (2010) could be accomplished. The freezer was altered in order to carry out the freeze and thawing cycles in an automatic sequence (Fig. 1a). For this, an electric resistance, a water agitator and a ventilator was added to the freezer. The electric resistance enables to increase the temperature until a value that is compatible with the standard, the water agitator enables to have the water, where the specimens are immersed, with uniform temperature and the ventilator enables both the internal environment temperature uniform and the renovation of air, see Fig.1b. The freezer (see Fig. 1c) is also equipped with a pump to empty and fill the chamber with water, where the specimens are stored, and with a heater for heating the water in the defrost phase. Two temperature sensors were considered to measure the internal environmental temperature of the freezer and the environmental temperature outside the freezer, so that it was possible to assess that the internal environment of the freezer was completely independent of the outside environment conditions. Additionally, a control temperature sensor was installed in the center of a control granitic specimen to monitor the continuous evolution of the temperature inside the specimen, and compare it with the internal environment temperature. This reference specimen enables to validate the test procedure defined with the adapted equipment, according to the values stipulated by European standard EN 12371 (2010) shown in Table 2. It was also seen that temperature sensors inside the freezer and inside the control specimen showed coincident readings.

A labview software (Fig.1d) application was developed to: (1) control the temperature in the freezer and make the sequence of the freeze-thawing cycles possible; (2) record the temperatures of the control sensors (Fig. 1c and Fig. 1d). According to the standard EN 12371

(2010), the freezing and thawing of the stone specimens should have a duration of 6 hours each, see Table 2. The labview software application addresses the computational cycles automatically, controlling the cycles of icing and thawing during 6 hours (21600 seconds) each, being also accounted the time to empty the chamber (beginning the cycle of ice when the samples are subjected to temperatures between 0ºC and -12°C), and the time to fill the recipient to fully immerse the specimens in water at a temperature between +5°C and +20ºC (starting of the defrost cycle), whose duration is 150 seconds. In this process, the temperature inside the freezer and the temperature inside the control specimen are recorded. Table 2 shows the temperature values required by the standard to which the specimens should be subjected. Preliminary tests were carried out to validate the testing procedure, being necessary to make some adjustments to obtain temperature readings within the required intervals.

The software developed to control the freeze-thaw cycles records automatically files related to the monitoring of the temperature in the control sample, inside the chamber and the outside atmosphere (ambient temperature). Fig. 2 shows the typical diagram with the evolution of the temperature in the center of the control specimen during 12 hours. It is seen that in the thaw cycle the temperature is reached in a very short time due to the introduction of water in the recipient and it is kept practically constant during 6 hours. In the freezing cycle, the decreasing in the temperature is more progressive but it is possible to accomplish the target temperatures at the times required by the European standard with slight small variations. Notice that the imposition of the freezing in the specimens is carried out after the water is taken out the recipient and it is promoted with the low air temperature that circulates in the freezer.

Testing procedures

As already mentioned, the freeze-thaw tests on the specimens were carried out according to the European standard EN 12371 (2010). Cubic specimens (70x70x70 cm) were adopted according to the recommendations about the geometry and dimensions of the specimens described in

the European standard EN 12371 (2010). A total of 28 specimens, 4 for granite PTM, 8 for granite MDB and 16 to the granite FT were tested to the action of freeze-thaw cycles. Notice that two loading directions were considered for the granite MDB, namely in the perpendicular and parallel directions to the foliation plan. Even if the EN 12371 (2010) indicated a maximum number of 240 freeze-thaw cycles if any of the damage thresholds is achieved, a total of 334 freeze-thaw cycles were considered in this work so that the damage progress could be recorded for a longer period. In Portugal, the freeze-thaw cycles occur essentially at the northeastern region, where temperatures reach values below -8°C during the night and reach values above 5ºC during the day. This daily temperature amplitude causes daily freeze-thaw cycles. Analyzing the meteorological data of the last three years and considering the most serious situation for Portugal (northeastern region), the temperature variations imposed by the European standard EN 12371 (2010) occur, in average, in approximately 8 annual days, meaning that 8 freeze-thawing cycles per year are imposed (Institute of Meteorology of Portugal 2011-2013). Taking this into account, it can be said that the effect of the 334 freeze-thaw cycles considered herein relate to the effect for a useful life of stone buildings of about 42years. Notice that, however, the conditions of the freeze-thaw tests are different from the ones occurring in real in-situ conditions, meaning that this equivalence should be seen with care.

Methodology to assess the deterioration of granites

In accordance to the European standard EN 12371 (2010), the assessment of the damage progress of the specimens submitted to freeze-thawing cycles should be made through: (1) visual inspection; (2) the variation of the dynamic modulus of elasticity; (3) the variation of the apparent volume. All control measurements were made after defrosting period (after the immersion of samples in water for 6 hours) according to the recommendations of EN 12371 (2010). The determination of changes in the apparent volume during cycles of freezing-thawing

allows accounting for the losses of material due to the deterioration experienced by the samples. It is considered that the deterioration of the specimens completes when the reduction in apparent volume, calculated according to European standard EN 12371 (2010), reaches 1% of the original apparent volume.

For the assessment of the variation on the dynamic modulus of elasticity during the freezing-thawing cycles, it was decided to measure the progress of the ultrasonic pulse velocity. Through the determination of the dynamic modulus of elasticity during cycles of freezing-thawing it is possible to detect internal deterioration associated to the appearance of microcracks and voids. A sample is considered deteriorated when the reduction in the dynamic elastic modulus reaches 30% in relation to the value measured at the initial state. As indicated by ISRM (1977) suggested methods, the dynamic modulus of elasticity (E_d) can be determined according to the eq. 1:

$$E_d = \rho \times C_p^2 \times 10^{-9} \text{ (GPa)} \quad (1)$$

Where ρ is the stone density in kg/m^3 and C_p is the ultrasonic pulse velocity (P-waves) in m/s.

The ultrasonic pulse velocity is also a useful method to provide information about the homogeneity of materials and detection of possible cavities and cracks in the internal structure. According to several authors (Popovics S. and Popovics J., 1997; Qasrawi, 2000; Turgut, 2004; Vasconcelos et al., 2008), the damage progress of granites, inducing alteration of the internal structure of the material, may be reasonably evaluated by the ultrasonic pulse velocity. The ultrasonic pulse velocity is affected by the moisture content of the material. As reported by Wang et al. (1990), the compressional wave velocities exhibit distinct values according to the different pore fluid present in the rock, and saturation increases compressional velocities. Similar results were pointed out also by Kahraman (2008) and by Vasconcelos et al. (2008). This is the reason by which the ultrasonic pulse velocity should be obtained in dry specimens.

255 Thus, besides the calculation of the dynamic modulus of elasticity, it was decided to analyze
256 the variation of the UPV in a qualitative approach and, to certain extent, to correlate it with the
257 observed deterioration. The ultrasonic testing was carried out in accordance with the European
258 standard EN 14579 (2004). For the ultrasonic pulse velocity measurements piezoelectric
259 transducers of 54KHZ were used. To measure the ultrasonic pulse velocity, it was necessary to
260 previously dry the samples until reach constant mass. The samples were then re-immersed in
261 water for 48 hours before restart the freeze-thaw cycles to ensure its saturation state for the next
262 ice cycle.

263 Visual inspection of the specimens is a fast, economical and easy method to assess the
264 superficial textural changes on the granites. After the freeze- thawing cycles, all the faces of the
265 specimens were examined carefully and classified according to the scale suggested in the
266 European standard EN 12371 (2010): (0) intact specimen; (1) very little damage (small
267 rounding of corners and edges) that do not compromise the integrity of the specimen; (2) one
268 or several cracks (<0,1mm wide) or detachment of small fragments (≤10mm^2 by fragment); (3)
269 one or several cracks, holes or detachment of small fragments superior to those defined for
270 classification "2", or alteration of the material contained in grains; (4) specimen broken in two
271 or with large cracks; (5) specimen broken into several pieces or disintegrated. A sample is
272 considered deteriorated when reaches classification "3".

273

274 *Physical and mechanical characterization*

275 Complementary to the damage indexes indicated in the European standard EN 12371 (2010) to
276 assess the deterioration process due to freeze-thaw cycles, it was decided to evaluate the
277 variation of the physical and mechanical before and after the freeze-thaw cycles. The physical
278 properties were obtained for each control point and the mechanical properties under uniaxial
279 compression were obtained before and after the completion of the freeze and thaw cycles.

280 The physical characterization of granites included the obtaining of the key physical properties,
281 such as porosity, the water absorption coefficient by immersion and capillary coefficient.
282 Capillary water absorption is one of the most significant physical properties of natural stone.
283 Capillarity occurs due to a process of suction water through the rock as water progresses often
284 from the soil by capillary rising. The network of pores in the structure of granites influences the
285 suction capacity and subsequent penetration of water and chemical substances. The negative
286 influence of water in many physical and mechanical properties of stone is well known (Almeida,
287 2000; Costa, 2009). The freeze-thaw cycles change the microstructure of the materials,
288 influencing its strength and frost resistance. The quantity of capillary water absorption and its
289 retention in the pores has a significant impact on the durability of individual varieties of
290 natural stone. If the absorbed capillary water is retained for a longer period of time at
291 temperatures lower than 0ºC, ice crystallizes. With the growth of ice crystals and the increased
292 volume of the ice, the durability can be significantly reduced. For these reasons, physical
293 properties were calculated before and after the selected control freeze-thaw cycles. The
294 coefficient of water absorption was determined based on the European standard EN 13755
295 (2008) and capillary absorption of water at atmospheric pressure was determined in accordance
296 of EN 1925 (1999) standard. The porosity of the samples was obtained in accordance with the
297 procedures given in ISRM suggested methods (1981) and in EN 1936 (2007) standard. The
298 samples after the defrost phase were saturated by water immersion in a vacuum of less than
299 800Pa for a period of two hours, to eliminate the air contained in the pores, and after this its
300 saturated-surface-dry mass, M_{sat}, was determined. The grain mass, M_s, is defined after oven
301 drying at a temperature of 70ºC. The apparent volume of the samples, V, is calculated as:

302 $$V = \frac{M_{sat} - M_{sub}}{\rho_w} \quad (2)$$

303 where M_{sub} is the saturated-submerged mass and ρ_w the water density.

304 The volume of open pores, V_v, is equal to:

$$V_v = \frac{M_{sat} - M_s}{\rho_w} \quad (3)$$

The open porosity (or apparent porosity), *n*, is the ratio between the volume of open pores and apparent volume of the specimen (expressed in percentage):

$$n = \frac{V_v}{V} \times 100 \quad (4)$$

The uniaxial compression tests were carried out to evaluate the deterioration degree of the specimens promoted by the freeze-thaw cycles, based on the decrease on the compressive strength and modulus of elasticity. Cubic samples (70×70×70mm^3) of each type of granite were tested before and after 334 freeze-thaw cycles. The uniaxial compression tests were carried out in a very stiff frame connected with an appropriate closed-loop control system, see Fig. 3a, at the Structural Laboratory of University of Minho. For the correct adjustment of the specimen to the upper steel plate, cubic steel pieces with the area of the sample surface were used to allow the adequate alignment of the applied force, see Fig. 3b. The axial displacements were recorded by means of three linear variable differential transformers (LVDT) located in three sides of the specimen, according to the disposition indicated in Fig. 3b. These LVDTs have a linear field of 10mm with a resolution of 0.05%. The elastic modulus was calculated as the slope of the tangent line up 30% of the maximum compressive strength (Fairhurst and Hudson, 1999).

Experimental results

The analysis of the damage progress resulting from the freeze-thawing cycles is carried out based on the standard damage indexes suggested in the European standard and complementary based on the variation of the ultrasonic pulse velocity, physical and mechanical properties. The damage control due the freeze and thaw was performed at 0, 34, 74, 104, 136, 178, 224, 258 and 334 freeze-thaw cycles.

Assessment of the standard damage indexes

The standard damage indexes are composed by the variation of mass, variation of the dynamic modulus of elasticity, complemented with a damage scale defined through visual inspection. Fig. 4a presents the mass loss during freezing-thawing cycles and Fig. 4b shows the decrease of the apparent volume along the control cycles. It is observed that from 0 to 74 cycles the mass loss in granite PTM ranges between 0.4g and 1.3g, representing a reduction of approximately 0.18% in the apparent volume. For the granite MDB the mass loss was about 1.8g, corresponding to a reduction of approximately 0.20% in the apparent volume. The granite FT lost in average 0.9g of material (reduction of 0.6% in apparent volume). In comparison to granites MDB and PTM, the granite FT is a more weathered due to the prolonged exposure to environmental conditions, contrarily to granites MDB and PTM whose origin was a quarry. This results in a higher degree of damage in the first cycles of freeze and thaw. After cycle number 74 up to cycle 224, the loss in all specimens is higher, reaching values ranging from 2g up to 3g (reduction in apparent volume between 0.6% up to 0.95%).

In the last freeze-thaw cycle, the granite MDB showed a decrease in apparent volume of 3.0% (reduction of 3.1g in mass), the granite PTM presented a variation of 2.50% (reduction of 2.6g in mass), and granite FT presented a reduction of the apparent volume of 2.4% (reduction of 3.1g in mass). In all cases, the reduction of the apparent volume is higher than 1%, as required by the European standard EN 12371 (2010) for the specimens to be considered damaged.

The variation of the ultrasonic pulse velocity and the variation of the dynamic modulus of elasticity calculated according to ISRM (1977) are shown in Fig. 5a and Fig. 5b, respectively. The reduction of the dynamic modulus of elasticity appears to be coherent with the increase on the mass variation. The specimens show a significant drop in dynamic elastic modulus after the freeze-thaw cycle number 74, decreasing in the range of 10% to 15% when 136 freeze-thawing cycles are completed. The reduction on the dynamic modulus of elasticity (DME) reached values close of 30% in the last freeze-thaw cycle. It is noteworthy that in average the specimens

353 showing higher reduction of the apparent volume (MDB and PTM), achieved a decrease in the
354 value of the dynamic modulus of elasticity between 25% up to 28% in the last cycle number
355 334. However, according to the criterion described in EN 12371 (2010) relatively to the
356 variation of the dynamic modulus of elasticity, only the granite FT can be considered degraded,
357 since it reached a reduction over 30% on the dynamic modulus of elasticity.
358 The ultrasonic pulse velocity measured during the freeze-thaw cycles decreases progressively
359 as the number of cycles increases. In the last cycle, the ultrasonic pulse velocity is, in average,
360 14%, 10% and 21% lower than the initial values for the granite PTM, MDB and FT,
361 respectively. These results are in line with the results found by other reserachers pointing out a
362 decrease of the ultrasonic pulse velocity in more weathered rocks as the result of freeze-thaw
363 cycles comparatively with healthy rocks (Iliev, 1966; Matsuoka, 1990; Matsuoka, 1991). The
364 decrease on the ultrasonic pulse velocity, which reflects also the decrease in the dynamic
365 modulus of elasticity, is associated to the alteration in the microstructure of the granites, due to
366 weathering resulting from the freeze-thaw cycles. The loss of surface grains, formation of
367 cracks and fissures (void formation) leads to the increase in the time of propagation of the
368 ultrasonic waves, with a consequent reduction in its propagation velocity. From the evolution
369 of ultrasonic pulse velocity shown in Fig. 5a, it is also possible to compare the behaviour among
370 the distinct granites due to the degradation induced by the freeze-thaw cycles: (1) the more
371 weathered granite in the initial state (granite FT) appears to experience a higher degree of
372 internal changes; (2) the different values of the ultrasonic pulse velocity on the granite MDB
373 results from the orientation according to which it is measured, namely in the direction parallel
374 and direction perpendicular to the foliation plane. However, it should be noticed that the
375 decreasing observed in the two directions measured presents the same trend.
376 Table 3 sets out the results obtained from the visual inspection for each freeze-thaw control
377 cycle. This inspection revealed some degree of wearing at the surface, particularly in granites

MDB and FT, see Fig. 6. In the last cycle, the specimens presented significant changes with detachment of small fragments at the corners, and according to the European standard EN 12371 (2010), they can be considered degraded as it was considered that the damage observed can be included in the degradation index of 3.

Assessment of the variation of the physical properties

In this section, an analysis of the variation of the physical properties with increasing number of freeze-thaw cycles is provided, namely: (1) variation of the porosity; (2) variation of the water absorption by immersion; (3) variation of the water absorption by capillary. The variation of the physical properties can give an indication about the changes on the internal structure induced by the damage associated to the freeze-thaw cycles. The variation on the porosity takes a central role, because its increase is directly related to the development of voids and internal microcracks due to the freeze-thaw induced damage. The increase on the porosity should result also in changes in the behavior of granites against water, which is related to several pathologies seen in the granites, namely formation of fungi and higher vulnerability to the salt attack.

The initial average values found for the porosity for granites MDB, PTM and FT cycle were respectively 4.10%, 3.95%, and 4.55% (see Table 1). The initial higher porosity of the granite FT is attributed to its higher degree of aging due to the environmental conditions, given that the granite specimens were taken from stones used in construction for long time. From the variation of the values of porosity shown in Fig. 7, it is seen that an important increase on the porosity was found after the completion of 34 freeze-thaw cycles and progressively increased for the subsequent freeze-thaw cycles. However, the increase on the porosity in less pronounced after the freeze-thaw cycle number 178 until the completion of the tests (334 cycle). It is seen that the scatter found for the granite FT is much higher, when compared to the granites PTM and MDB. This should be associated to the weathering process developed in the stone during the years as the specimens were cut from different stones. At the end of the freeze-thaw cycles, the

403 porosity of the granites MDB, PTM and FT is 5.30%, 4.89% and 6.10% respectively,
404 corresponding to an increase on the porosity of about 24% for the PTM specimens, 31.5% for
405 the MDB granite and 34% for the FT granite. This result indicates that the damage due to the
406 freeze and thaw cycles was higher in granite FT. The mass loss analyzed previously is related
407 to the disaggregation of the material. This means that the imposition of freeze-thaw cycles to
408 the granites reduced the dry mass and consequently increased the porosity. The direct relation
409 between the loss on dry mass and the increase on the porosity is shown in Fig. 8, through the
410 linear correlation found between both variables, which, despite the scatter, presented a
411 reasonable coefficient of correlation.

412 The increase on the porosity is directly associated with the higher values of water absorption
413 by immersion and capillary. As shown in Fig. 9a the water absorption by immersion increased
414 after the freeze-thaw cycles ranging in average from 1.47% up to 1.97% for granite PTM, from
415 0.79% up to 2.30% for the granite MDB and from 1.84% up to 2.52% for the granite FT. The
416 variation of the water absorption by immersion presents a nonlinear evolution, being the rate of
417 increase higher in the earlier freeze-thaw cycles and much lower in case of the last cycles,
418 similarly to the trend observed for the variation of porosity. With respect to the water absorption
419 by capillarity, the values were increased during the freeze-thaw cycles in accordance with the
420 diagram of Fig. 9b. Contrarily to the increasing nonlinear trend observed with regard to the
421 water absorption by immersion, the water absorption by capillary exhibits a linear increasing
422 trend.

423 It is also observed that the increase on the capillary coefficient during the freeze-thaw cycles is
424 more pronounced in case of the granite FT. The maximum absorption capillary coefficient
425 obtained after the last cycle is 0.362 $g/cm^2h^{1/2}$ in granite FT, followed by granite MDB with
426 0.231 $g/cm^2h^{1/2}$ and finally by the granite PTM with a capillary coefficient of 0.174 $g/cm^2h^{1/2}$.
427 Before the freeze-thaw cycles, these granites exhibited an initial value for the absorption

coefficient of 0.264 g/cm^{2}h$^{1/2}$ (FT), 0.164 g/cm^{2}h$^{1/2}$ (MDB) and 0.127 g/cm^{2}h$^{1/2}$ (PTM), meaning that variations of about 27.1%, 29% and 27% were found for granites FT, MDB and PTM respectively. The difference found in the water absorption by capillary can be also seen in Fig. 10, where the curves of water absorption by capillarity versus the square root of time before and after the completion of freeze-thaw cycles are presented. Besides the increase on the slope of the linear range, reflecting the increase on the water absorption capillary coefficient, it is possible to notice the decrease on the scatter in the linear range. It is interesting to notice also that after the completion of the freeze-thaw cycles, there is a more clear separation between the capillary curves between granite PTM and granite MDB, which may indicate that the weathering induced process becomes the internal porosity more homogeneous. Similarly to what was found for porosity, the increase of the water absorption by immersion and by capillary, which results from the material degradation, results from the mass loss during the action of freeze and thawing. A linear correlation was found between the dry mass loss and the increase on the water absorption and capillary absorption, as shown in Fig. 11a and Fig. 11b, respectively. It is observed some scatter characterizes these statistical correlations but the coefficient of correlation is considered to be reasonable.

Assessment of the variation of the mechanical properties

The diagrams regarding the relation between uniaxial compressive strength and strain obtained in the uniaxial compressive tests on cubic specimens before and after the freeze–thaw cycles are shown in Fig. 12. Besides, the average values found for the compressive strength and for the elastic modulus are summarized in Table 4. From this data it is observed that the initial uniaxial compressive strength was 79.03 MPa for the granite MDB-P in the perpendicular direction to foliation, 77.27 MPa for the granite MDB in the parallel direction to foliation, 87.90 MPa for the granite PTM and 45.67 MPa to the granite FT. These results show that the compressive strength of granite FT is clearly lower than the values found for the other granites,

453 due its higher degree of initial weathering and higher initial porosity. The compressive strength
454 obtained after 334 freeze-thaw cycles was about 46.11MPa for granite MDB in the
455 perpendicular direction to foliation, 54.26MPa for the granite MDB in the parallel direction to
456 foliation, 69.83MPa for granite PTM and 39.40MPa for granite FT, corresponding to a lowering
457 of about 37%, 21% and 14% respectively for granite MDB, granite PTM and granite FT.
458 Relatively to the elastic modulus, the reduction is less pronounced for granites MDB and PTM
459 (23.5% and 11% respectively) but higher variation was found for granite FT with an average
460 decreasing of about 34%. It should be noticed that the induced damage due to the freeze-thaw
461 cycles led to the considerable increase on the scatter of the force-displacement diagrams,
462 resulting naturally in the higher scatter of the mechanical properties.
463 The crack patterns of the granites results from splitting in slice shapes. From the comparison of
464 the failure modes observed in the cubic specimens before and after the freeze-thaw cycles it is
465 seen that any clear change was observed , see Fig. 13 and Fig. 14. Similar results were pointed
466 out by Tan et al. (2011), which investigated the influence of the freeze-thaw cycles on the
467 mechanical properties of granites.
468
469 **Concluding remarks**
470
471 Natural stones are generally used as building materials for construction and ornamentation.
472 Aiming at assessing the degradation process of granitic stones due to the freeze-thaw action, a
473 laboratory experimental campaign was designed based on physical and mechanical tests and on
474 freeze-thaw cycles. The damage indexes suggested by European standard were analysed,
475 namely the variation on the apparent volume, the variation on the dynamic modulus and the
476 damage characterization based on visual inspection. Additionally, the variation of physical and
477 mechanical properties (compressive strength and modulus of elasticity) before and after freeze-
478 thaw cycles was analysed.

Based on the results of the experimental campaign on the freeze-thaw cycles on the three distinct types of granites, it was observed that all the criteria suggested by the EN 12371 (2010) to characterize the degradation are sensitive and can be used as damage indexes. In fact, both dynamic modulus of elasticity and variation on the apparent volume varies considerably during the sequence of freeze-thaw cycles. However, it should be noticed that the granites under study are considered deteriorated for greater number of freeze-thaw cycles, particularly in case of granite PTM and granite MDB. Even if great part of the specimens of granite FT can be considered deteriorated after 136 freeze-thaw cycles in terms of variation of the apparent volume, in case of the dynamic modulus and visual inspection only after the 258 cycles these criterion was accomplished. For the granites MDB and PTM, the specimens reached the deterioration after 258 freeze-thaw cycles: (a) variation on the apparent volume higher than 1%; (b) damage index defined by visual inspection equal to 3 in the scale from 0 to 5; (3) decrease on the dynamic modulus of elasticity close to 30%. It should be stressed that the granites under study present a higher initial porosity, meaning that in fresh granites with much lower porosity, it is feasible that deterioration cannot be achieved for the maximum number freeze-thaw cycles of specimens suggested by the European standard.

The freeze-thaw cycles showed to have a considerable influence in the physical and mechanical properties of granites: (1) the ultrasonic pulse velocity progressively decreased in all samples after the freeze-thaw cycles following a linear decreasing trend. The decreasing was more pronounced in the granite with higher initial porosity; (2) the dynamic elastic modulus calculated based on ultrasonic pulse velocity also decreased with increased number of freeze-thaw cycles; (3) the dry mass varied as a result of the detachment of material and alteration of the internal structure of granite. The reduction on the dry mass resulted in the variation of the apparent volume; (4) the granites present a considerable increase on the porosity after the freeze-thaw cycles ranging from 24% (granite PTM) to 34% (granite FT); (5) the increase on

the porosity also leads to the increase on the absorption by immersion and on the capillary absorption coefficient; (6) the uniaxial compressive strength and, particularly, the elastic modulus decrease after the last freeze-thaw cycle considered (334).

Additionally, it was observed that, generally, specimens with greater visible surface damage were those with greater mass reduction and greater variation on porosity. The ultrasonic pulse velocity demonstrated also to be a good indicator about the deterioration of the granitic specimens induced by the freeze-thaw cycles. A linear decreasing trend was observed for the three distinct types of granites, being the slope greater in the granite with higher porosity.

It should be stressed that the results of this investigation are limited to the granites under study, which can be found in several vernacular and historical ancient buildings in the northeastern region of Portugal. It is considered that further results are needed to understand better the influence of the freeze-thaw cycles in other types of granites, namely in the granites with lower porosity and, thus, lower levels of initial weathering. It is also considered important to extend the present study to other types of building stones as it is believed that the degradation evolution due to the freeze-thaw cycles is dependent on the internal structure of the materials. Additionally, the impact of the freeze-thaw cycles on the physical properties should be also different in distinct types of building stones.

Acknowledgements

This work has been financially supported by the research project Seismic V- Vernacular seismic culture in Portugal (PTDC/ATP-AQI/3934/2012), funded by the Portuguese Foundation for Science and Technology.

References

Almeida, F. (2000). Manual de Conservação de Cantarias. Instituto do Patrimônio Histórico e Artístico Nacional/Ministério da Cultura, 43.

Alomari, A., Brunetaud, X., Beck, K., and Al-Mukhtar, M. (2013). Freezing-thawing action in the deterioration of the stones of Chambord Castle. EGU General Assembly, 15.

Bayram, F. (2012). Predicting mechanical strength loss of natural stones after freeze–thaw in cold regions. Cold Regions Science and Technology 83-84, 98-102.

Benavente, D., García del Cura, M.A., Fort, R., and Ordónez, S. (2004). Durability estimation of porous building stones from pore structure and strength. Engineering Geology 74, 113-127.

Chatterji, S. (1999). Aspects of the freezing process in a porous material-water system. Part 1. Freezing and the properties of water and ice. Cemente and Concrete Research 29, 627-630.

Chatterji, S. (2000). A discussion of the paper Crystallization in pores by G. W. Scherer. Cement and Concrete Research 30, 669-671.

Costa, C. (2009). Análise numérica e experimental do comportamento estrutural de pontes em arco de alvenaria de pedra. Dissertação de Mestrado em Engenharia Civil, Faculdade de Engenharia Universidade do Porto.

EN 12371. (2010). Natural stone test methods. Determination of frost resistance. Brussels : European Committee for Standardization.

EN 14579. (2004). Natural stone test methods. Determination of sound speed propagation. Brussels : European Committee for Standardization.

EN 13755. (2008). Natural stone test methods. Determination of water absorption at atmospheric pressure. Brussels: European Committee for Standardization
.

EN 1925. (1999). Natural stone test methods. Determination of water absorption coefficient by capilarity. Brussels : European Committee for Standardization.

EN 1936. (2007). Natural stone test methods. Determination of real density and apparent density and total and open porosity. Brussels: European Committee for Standardization.

Exadaktylos, G. (2006). Freezing-thawing model for soil and rocks. Journal of Materials in Civil Engineering 18(2), 241-249.

Evans, I. (1970). Salt crystallization and rock weathering: a review. Revue de Géomorphologie Dynamique. Vols. XIX,4,153-177.

Everett, D. (1961). The thermodynamics of frost damage to porous solids. Trans. Faraday Society 57 (9),1541-1551.

Fairhurst, C.E., and Hudson, J.A. (1999). Draft ISRM suggested method for the complete stress-strain curve for intact rock in uniaxial compression. International Journal of Rock Mechanics and Mining Sciences 36, 279-289.

578 Gao, P., Wu, S., Lin, P., Wu, Z., and Tang, M. (2006). The characteristics of air void and frost
579 resistance of RCC with fly ash and expansive agent. Construction and Building Materials
580 20, 586-590.
581
582 Iliev, I. G. (1966). An attempt to estimate the degree of weathering of intrusive rocks from their
583 physico-mechanical properties. Proceedings 1st Congress of the International Society of
584 Rock Mechanics. Lisboa Vol.I, 109-114.
585
586 Institute of Meteorology of Portugal (2011-2013). Boletim Climatológico Sazonal de Inverno.
587
588 ISRM (International Society for Rocks Mechanics). (1977). Suggested methods for determining
589 sound velocity. In Brown, E.T.(Ed.), ISRM Suggested Methods. Pergamon Press, Oxford.
590
591 ISRM (International Society for Rocks Mechanics). (1981). Suggested methods for water
592 content, porosity, density, absorption and related properties and swelling and slake-
593 durability index properties. In Brown, E.T.(Ed.), ISRM Suggested Methods. Pergamon
594 Press, Oxford.
595
596 Kahraman, S. (2007). The correlations between the saturated and dry P-wave velocity of rocks,
597 Ultrasonics, 46(4) 341-348.
598
599 Martínez-Martínez, J., Benavente, D., Gomez-Heras, M., Marco-Castaño, L., and García-del-
600 Cura, M. (2013). Non-linear decay of building stones during freeze–thaw weathering
601 processes. Construction and Building Materials 38, 443-454.
602
603 Matsuoka, N. (1990). Mechanisms of rock breakdown by frost action: an experimental
604 approach. Cold Regions Science and Technology 17, 253–270.
605
606 Matsuoka, N. (1991). A model of the rate of frost shattering: application to field data Japan,
607 Svalbard and Antarctica. Permafrost and Periglacial Processes 2, 271-281.
608
609 Maurenbrecher, A.H.P., Trischuk, K., Subercaseaux, M. I., and Suter, G. T. (2005). Preliminary
610 evaluation of the freeze-thaw resistance of hydraulic lime mortars. RILEM workshop on
611 repair mortars for historic masonry.
612
613 Nicholson, D.T. (2001). Pore properties as indicators of breakdown mechanisms in
614 experimentally weathered limestones. Earth Surface Processes and Landforms 26 ed.
615
616 Popovics, S., Popovics, J. (1997). A critique of the ultrasonic pulse velocity method for testing
617 concrete. NDT and E International, 30(4), 260-260.
618
619 Powers, T. (1945). A working hypothesis for further studies of fros resistance of conccrete. ACI
620 Journal 41 (3), 245-272.
621
622 Pospíchal, O., Kucharczyková, B., Misák, P., and Vymazal, T. (2010). Freeze-thaw resistance
623 of concrete with porous aggregate. Procedia Engineering 2, 521-529.
624
625 Qasrawi H (2000). Concrete strength by combined nondestructive methods simply and
626 reliably predicted. Cement and Concrete Res., 30(5), 739-746.
627

628 Scherer, G. (2000). Reply to the discussion by S. Chatterji of the paper, "Crystallization in
629 pores". Cement and Concrete Research 30, 673-675.
630
631 Shang, Huai-Shuai, Song, Yu-Pu and Qin, Li-Kun (2008). Experimental study on strength and
632 deformation of plain concrete under triaxial compression after freeze-thaw cycles. Building
633 and Environment 43,1197-1204.
634
635 Tan, X., Weizhong, C., Yang J., Cao J. (2011). Laboratory investigations on the mechanical
636 properties degradation of granites under freeze-thaw cycles, Cold Regions Science and
637 Technology 68, 130-138.
638
639 Tugrul, A. (2004). The effect of weathering on pore geometry and compressive strength of
640 selected rock types from Turkey. Engineering Geology 75, 215-227.
641
642 Turgut, P. (2004). Research into the correlation between concrete strength and UPV values.
643 NDT. net, 12, 12.
644
645 Uddin, M., Mustapha, G., Mufti, A., and Thomson, D. (2010). Freeze-Thaw Durability of
646 Anchor Materials in Heritage Masonry Stones. 2nd International Structures Specialty
647 Conference,1-9.
648
649 Vasconcelos, G., Lourenço, P.B., Alves, C.A.S., and Pamplona, J. (2008). Ultrasonic evaluation
650 of the physical and mechanical properties of granites. Science Direct 48, 453-466.
651
652 Vegas, I., Urreta, J., Frías M., and García, R. (2009). Freeze–thaw resistance of blended
653 cements containing calcined paper sludge. Construction and Building Materials 23, 2862-
654 2868.
655
656 Wang, Z., Battle, M.L., Nur, A. (1990). Effect of different pore fluids on seismic velocities in
657 rocks, Canadian Journal of Exploration Geophysics, 26, 104-112.
658

Figures Captions

Fig. 1. Equipment for testing the freeze-thaw: (a) setup tests; (b) ventilator on the chamber lid; (c) automatic program and (d) detail of the interior of the chamber

Fig. 2. Monitoring of temperature at the center of the control specimen during the freeze thaw cycles

Fig. 3. Uniaxial compression test: (a) testing equipment (b) test setup

Fig. 4. Mass evolution during freeze-thawing cycles: (a) dry weight and (b) decrease of the apparent volume

Fig. 5. Ultrasonic pulse test: (a) evolution of UPV; (b) variation of dynamic modulus of elasticity

Fig. 6. Damage characterization in the process of freeze-thaw cycle 334 through visual inspection: (a) wear along the edge of the sample MDB; (b) detachment of a corner portion of the sample PTM and (c) wear along the edge of the FT sample

Fig. 7. Porosity vs. number of freeze–thaw cycles

Fig. 8. Relation between weight loss and porosity

Fig. 9. Behavior of granites to water during the freeze-thawing cycles; (a) water absorption by immersion and (b) water absorption by capillarity

Fig. 10. Behaviour of granites to water absorption by capillary: (a) before the freeze-thaw cycles and (b) after freeze-thaw cycles (last cycle number 334)

Fig. 11 Assessment of the influence of the weight loss in the physical properties; (a) water absorption by immersion; (b) water absorption by capillary

Fig. 12. Stress-strain relationship for uniaxial compression tests: (a) before freeze–thaw cycles (b) after last freeze–thaw cycle

Fig. 13. Typical failure modes for uniaxial compressive test before freeze–thaw cycles: (a) MDB samples, (b) PTM samples and (c) FT samples

Fig. 14. Typical failure modes for uniaxial compressive test after freeze–thaw 334 cycle: (a) MDB samples, (b) PTM samples and (c) FT samples

Tables List

687 **Table 1.** Description of granites under study

688 **Table 2.** Temperature values in the control sample required by the EN 12371 (2010) standard
689 for the testing of freeze-thaw

690 **Table 3.** Results of the visual inspection in specimens after each freeze-thawing cycles

691 **Table 4.** Average compressive strength and elastic modulus before and after o freeze–thaw
692 cycles. Coefficient of variation in brackets

693

694

695 **Table 1.** Description of granites under study

Granite Designation	Description	Mean length (mm)	Grain size range (mm)	Porosity (%)
MDB	Medium-grained two- mica granite	0.7-0.9	0.3-14.5	4.10
PTM	Fine to medium-grained two-mica granite	0.7-0.8	0.3-12.0	3.95
FT	Medium-grained two- mica granite	0.7-0.9	0.3-13.5	4.55

696

697

698 **Table 2.** Temperature values in the control sample required by the EN 12371 (2010) standard
699 for the testing of freeze-thaw

Procedure	***Temperature in center of the specimen***	***Time***
Cycle start	≥ + 5 ºC ≤ + 20 ºC	T_0
Phase 1	≤ 0 ºC ≥ - 8 ºC	T_0 + 2h
Phase 2	≤ - 8 ºC ≥ - 12 ºC	T_0 + 6h
Phase 3	Full immersion	T_0 + 6,5h
Phase 4	≥ + 5 ºC ≤ + 20 ºC	T_0 + 9h
Phase 5	≥ + 5 ºC ≤ + 20 ºC	T_0 + 12h

700

701

Table 3. Results of the visual inspection in specimens after each freeze-thawing cycles

Granite	Cycles								
	0	**34**	**74**	**104**	**136**	**178**	**224**	**258**	**334**
PTM	0	0	1	1	1	1	2	3	3
MDB	0	0	1	1	2	2	2	3	3
FT	0	0	1	1	1	2	2	3	3

(0) intact specimen; (1) very little damage (small rounding of corners and edges); (2) one or several cracks (<0,1mm wide) or detachment of small fragments (≤10mm2 by fragment); (3) one or several cracks, holes or detachment of small fragments superior to those defined for classification "2", or alteration of the material contained in veins; (4) specimen broken in two or with large cracks; (5) specimen broken into several pieces or disintegrated

707 **Table 4.** Average compressive strength and elastic modulus before and after o freeze–thaw cycles.
708 Coefficient of variation in brackets

Granite	Compressive strength (N/mm^2)		Elastic modulus (N/mm^2)	
	Before freeze-thaw	**After freeze-thaw**	**Before freeze-thaw**	**After freeze-thaw**
MDB-P	79.03(6%)	46.11(21%)	10538(11%)	7277(20%)
MDB-L	77.27(7%)	54.26(15%)	10545(6%)	9489(10%)
PTM	87.90(5%)	69.83(20%)	12386(15%)	11791(20%)
FT	45.67(12%)	39.40(18%)	4184(10%)	2763(20%)

709

710

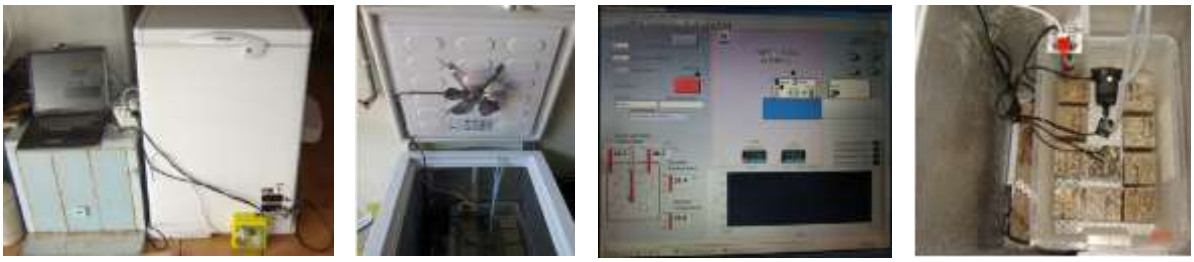

(a) (b) (c) (d)

711 **Figure 15.** Equipment for testing the freeze-thaw: (a) setup tests; (b) ventilator on the chamber lid; (c)
712 automatic program and (d) detail inside the chamber

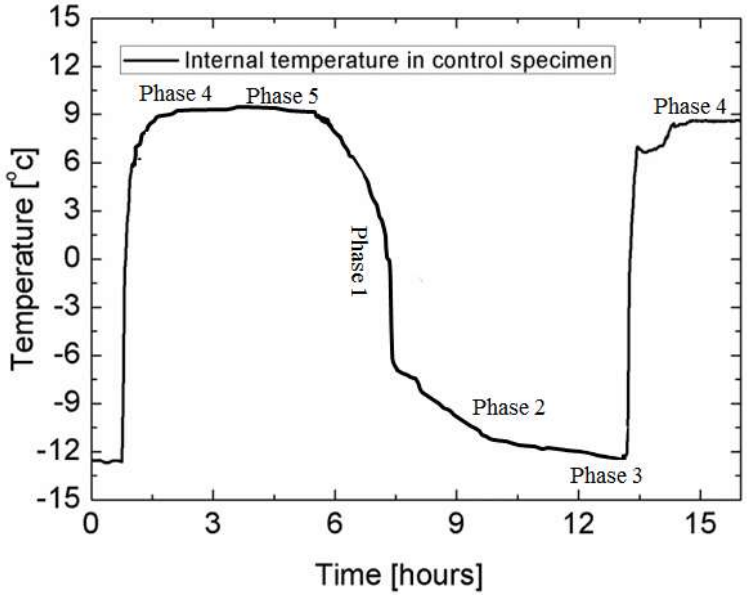

713

714 **Figure 16.** Monitoring of temperature at the center of the control specimen during the freeze-thaw
715 cycles

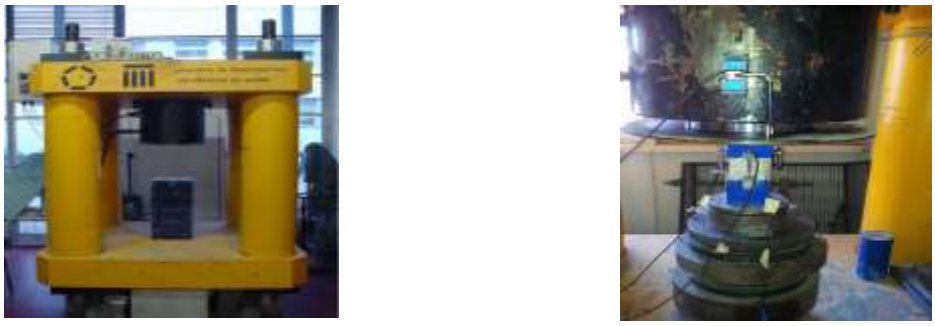

(a) (b)

716 **Figure 17.** Uniaxial compression test: (a) testing equipment (b) test setup

717

718

719

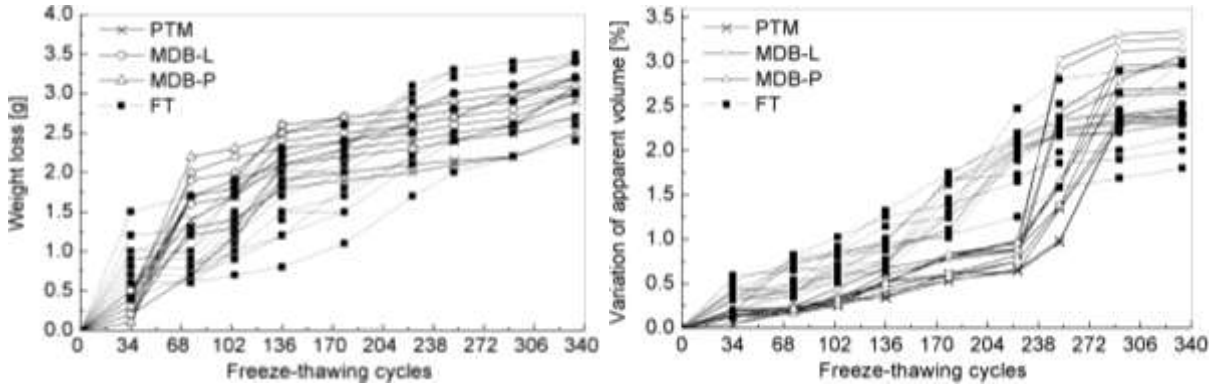

(a) (b)

720 **Figure 18.** Mass evolution during freeze-thawing cycles: (a) dry weight and (b) variation of the
721 apparent volume

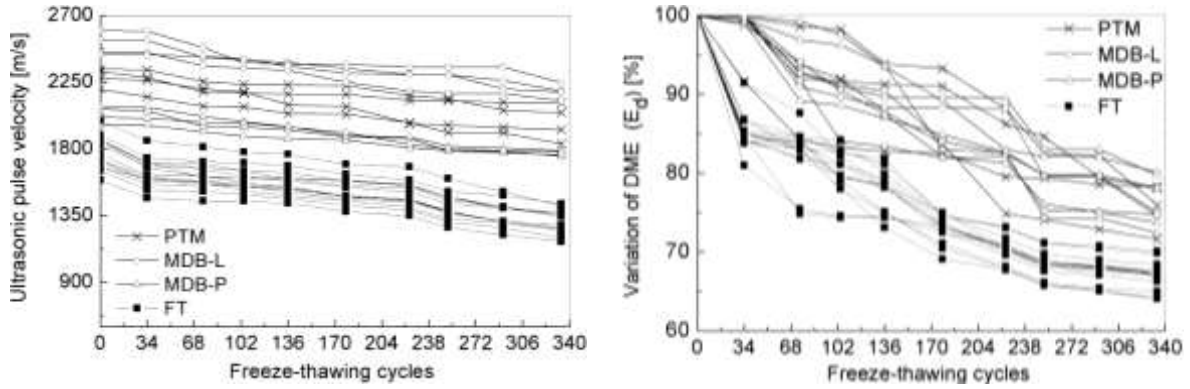

(a) (b)

722 **Figure 19.** Ultrasonic pulse test: (a) evolution of UPV; (b) variation of dynamic modulus of elasticity

723

(a) (b) (c)

724 **Figure 20.** Damage characterization in the process of freeze-thaw test through visual inspection: (a)
725 wear along the edge of the sample MDB; (b) detachment of a corner portion of the sample PTM and (c)
726 wear along the edge of the FT sample

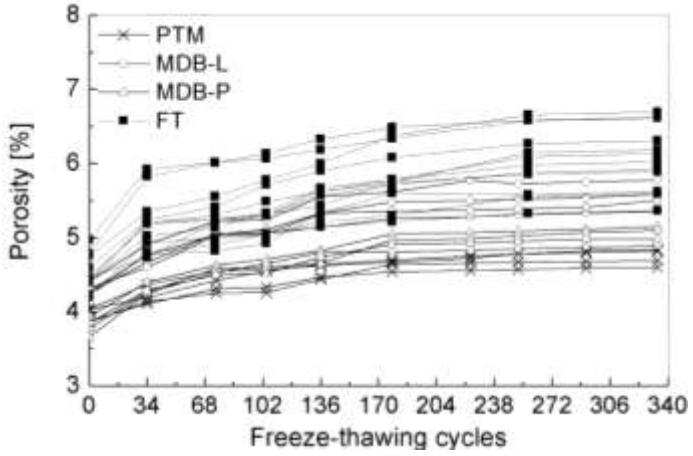

727

728 **Figure 21.** Porosity vs. number of freeze–thaw cycles

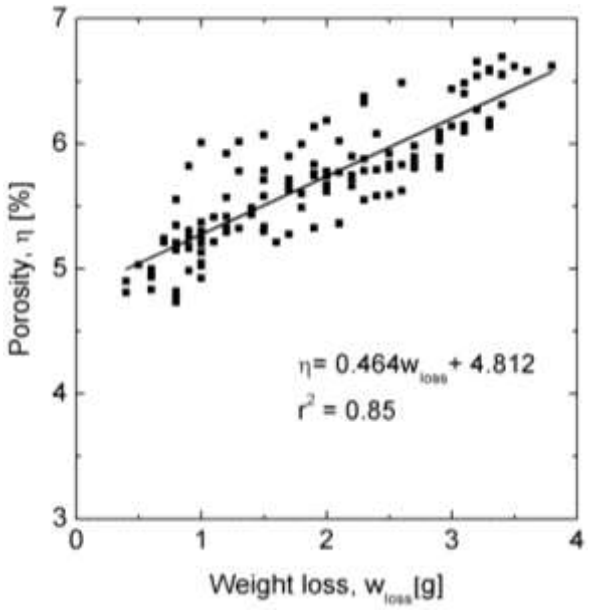

729 **Figure 22.** Relation between weight loss and porosity

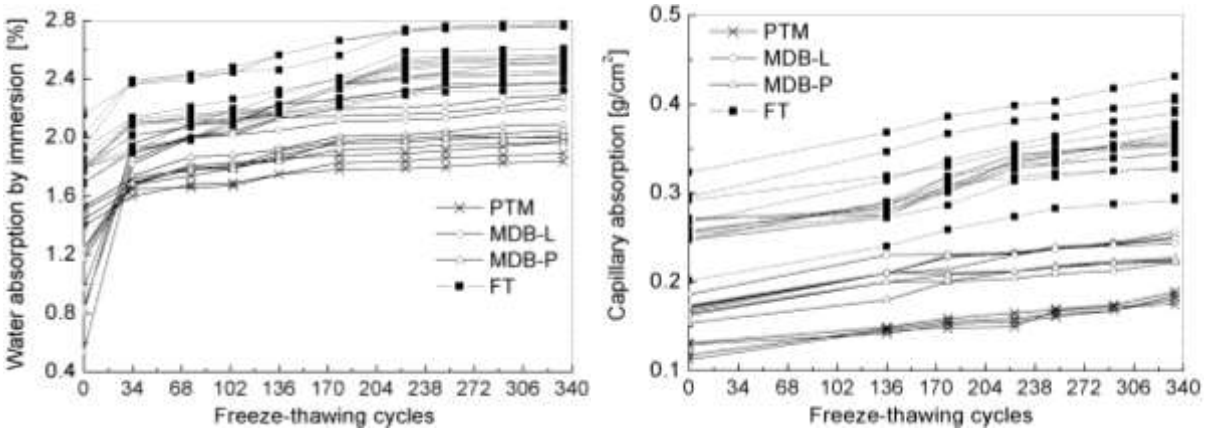

(a) (b)

730 **Figure 23.** Behavior of granites to water during the freeze-thawing cycles; (a) water absorption by
731 immersion and (b) water absorption by capillarity

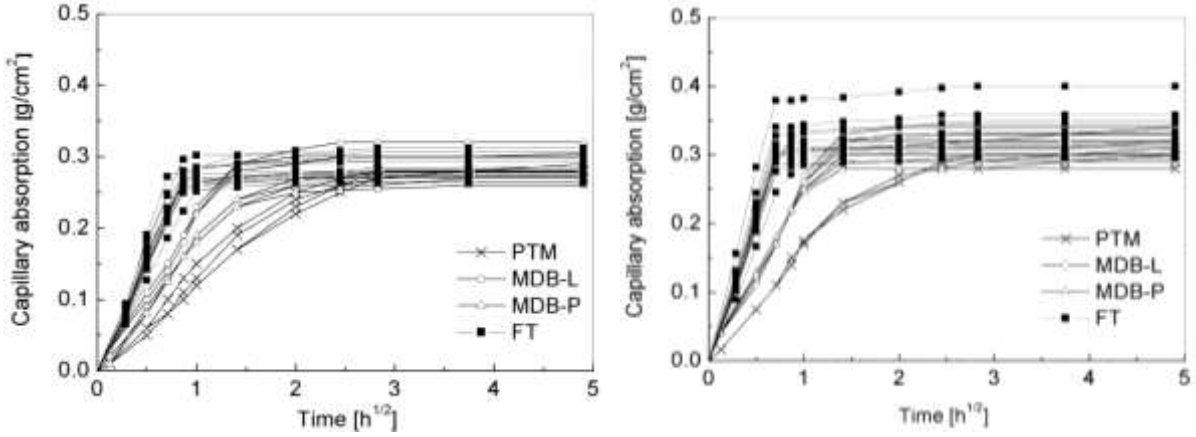

(a) (b)

732 **Figure 24.** Behaviour of granites to water absorption by capillary: (a) before the freeze-thaw cycles
733 and (b) after freeze-thaw cycles (last cycle number 334)

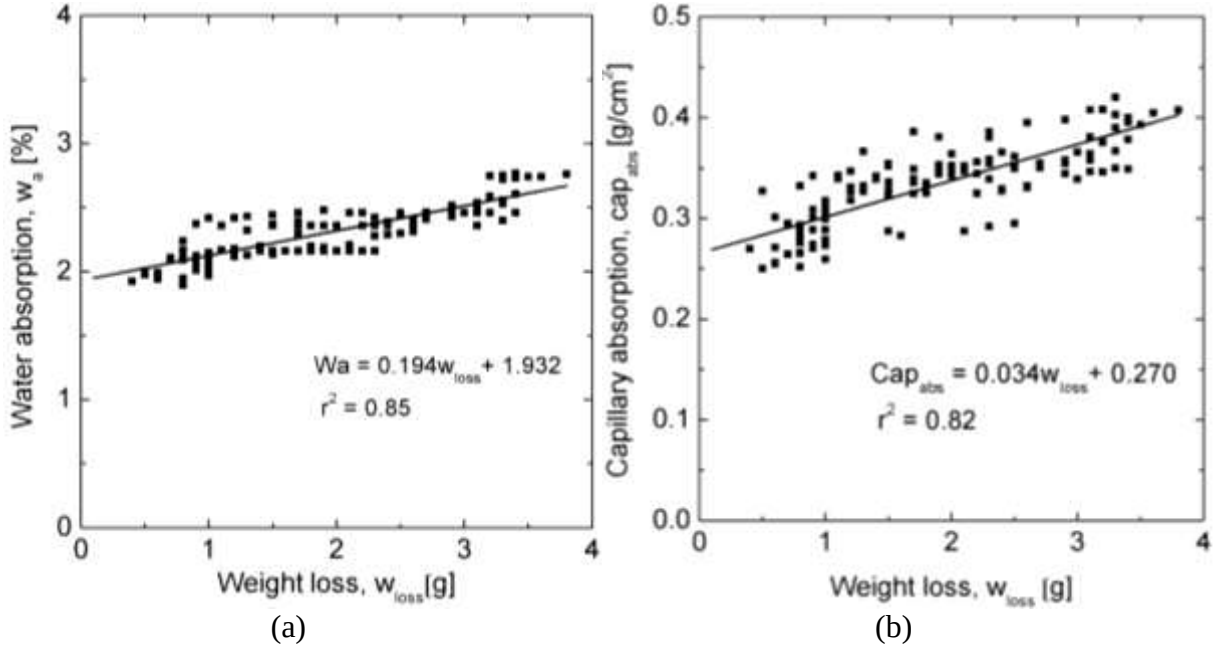

(a) (b)

734 **Figure 25** Assessment of the influence of the weight loss in the physical properties; (a) water
735 absorption by immersion; (b) water absorption by capillary

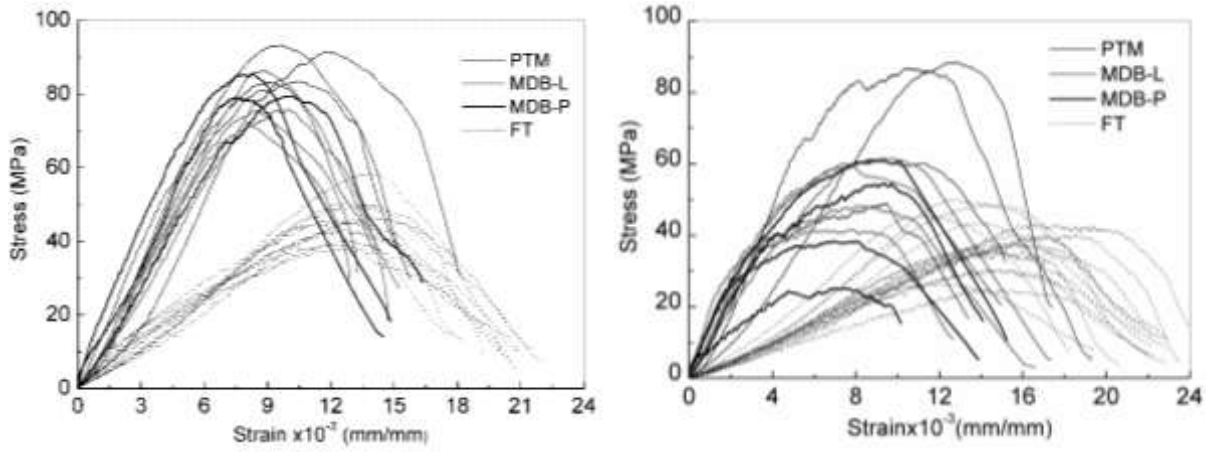

(a) (b)

736 **Figure 26.** Stress-strain relationship for uniaxial compression tests: (a) before freeze–thaw cycles (b)
737 after last freeze–thaw cycle

(a) (b) (c)

738 **Figure 27.** Typical failure modes for uniaxial compressive test before freeze–thaw cycles: (a) MDB
739 samples, (b) PTM samples and (c) FT samples

(a) (b) (c)

740 **Figure 28.** Typical failure modes for uniaxial compressive test after freeze–thaw cycles: (a) MDB
741 samples, (b) PTM samples and (c) FT samples

742

743